International Journal of Engineering Research And Management (IJERM)
ISSN : 2349- 2058, Volume-01, Issue-07, October 2014

An investigation about optical parameters of silicon thin layers with different thicknesses

Parshang Khorramdel, Mohammad Reza Behfrooz

***Abstract*— Silicon thin layers with different deposition angle were made by using of resistant evaporation method. These layers were deposited on glass substrates with three different thicknesses and angles, under UHV conditions at room temperature by electron gun evaporation method. Other deposition conditions were the same for all layers. By using spectrophotometer the Reflectance and the Transmittance of produced layers were obtained other deposition Conditions were the same for all layers. Nano Structure of these layers and their relation with deposition angle were discussed by applying AFM and SEM analysis.**

***Index Terms*— Silicon, thin layers, AFM and SEM analysis, Nano Structure**

I. INTRODUCTION

The development of soft condensed matter surfaces at the molecular level is nowadays believed to be the building blocks for the creation of the next generation of materials and devices in practically all scientific areas. Particularly the buildup of functional macromolecular hetero structures and mimic of biological structures are in fact an actual trend. The advances in soft condensed analysis matter surfaces are mostly related with the atomic force microscopy (AFM) which was introduced in 1986 [1] and originated with the invention of the scanning tunneling microscope in 1982 by Binning and Rohrer [2,3].The traditional approach to the backside metallization in semiconductor technology is the evaporation process ,where the target materials are contained in a crucible mounted at the bottom of a large vacuum chamber (Figure1).

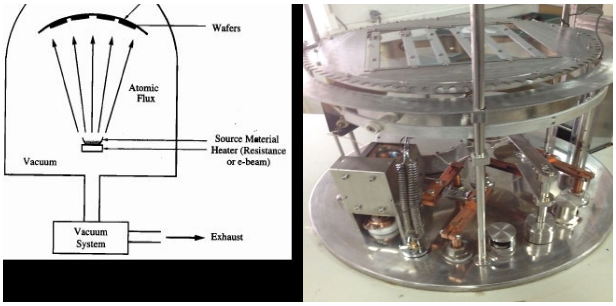

Figure 1: Scheme of principle of an evaporation system.

A beam of electrons is generated, accelerated and directed towards the crucible containing the material to be deposited [4]. Part of the surface melts and the material evaporates .The metal deposits itself on wafers mounted on a rotating cap (this configuration is named “planetary system”). Some of the basic advantages of this method are the high deposition rate and the low damage caused by the deposited atoms because of their low energy. Furthermore, the evaporation process is an inexpensive process. Many materials can be evaporated in one run, high throughput can be achieved for wafers with diameter up to 150mm (The throughput is determined by the number of possible wafers within one run. With increasing of the wafer diameter, the number of possible wafers mounted on the wafer holder is decreasing). The physical principle of the sputtering is the dislocation of atoms from the surface of a metal target. The dislocation of metal atoms is caused by the collision of high energy ions generated in magnetron assisted DC plasma. The ejected neutral atoms fly through the plasma and land on the wafer situated in the opposite side of the target [5], [6]. Silicon thin films are used in different technological areas such as photovoltaic cells, thin-film transistors, microelectromechanical systems, and Li-ion rechargeable batteries. Silicon dielectrics are important materials for both microelectronics and integrated optics. They have been considered as an appropriate material for fabricating optical waveguides in broadband communications (telecom and datacom) [7]. Silicon is very important material in electronics market, dominating the microelectronics industry with about 90% of all semiconductor devices sold worldwide being silicon based [8]. Currently, the vast majority of flash-memory devices are charge storage based, fabricated in CMOS technology. Because of the increasing demand for information storage, memory device developers and manufacturers are constantly attempting to increase storage capacity for memory devices (e.g., increase storage per die or chip). Silicon-based devices are approaching their fundamental physical size limits [9]. The aim of this work is to study the relation between optical properties of silicon thin films and their thicknesses.

II. EXPERIMENTAL DETAILS

Silicon nanolayers were perepered on glass in 2.5×7.6 and thickness of 1-1.2 mm.we using an ETS160 system with 2.9×10^{-5} m bar pressure .First we wash those lamina by substratum bath for 15 minutes in pure acetone and 15 minutes in absolute alcohol, then we I located (the grey powder of Si) on the top of the tungsten boat .The temperature of substrates was kept constant (300 K). The thicknesses of the layers were 91.9,119 and 173nm .As we know the layers that was vertical has thick layer than the others (25 and 35 degree).

Manuscript received Sep 10, 2014

Parshang Khorramdel, Department of Atomic and Molecular Physics, Science and research branch, Eslamic Azad University, Tabriz, Iran
Mohammad Reza Behfrooz, [2]Department of Atomic and Molecular Physics, Eslamic Azad University, Mahabad, Iran

On the experiment Silicon thin layers with different deposition angle were made by using of resistant evaporation method. Other deposition conditions were the same for all layers. Nanostructure of these layers and their relation with deposition angle were discussed by applying AFM and SEM analysis.

III. RESULTS AND DISCUSSION

As we can see in figure 1 is high levels of fine grained needles with empty spaces between them, and the coarseness of about 91.9 nm by reducing the accumulation of seed 25 degree angle to the substrate more stacked silicon.

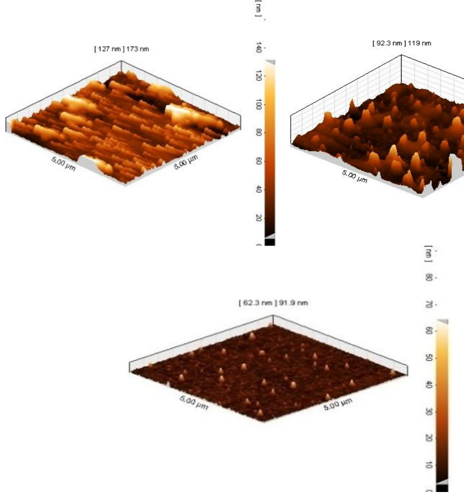

Figure3 Figure 2 Figure 1

If there is a decrease in the angle accumulation of more grains accumulate on the surface of the substrate and the seeds with the tip of tiny dome and coarse grains with and the given the number of pores between them dropped. Coarseness is 91.9 nm.

As we can see in Figure 3 grains growth under the influence of the mass clusters become large surface silicon layer is covered. Coarseness of the surface is about 119 nm. It should be noted that the deposition temperature is room temperature in both tests so we cannot see surface distribute.

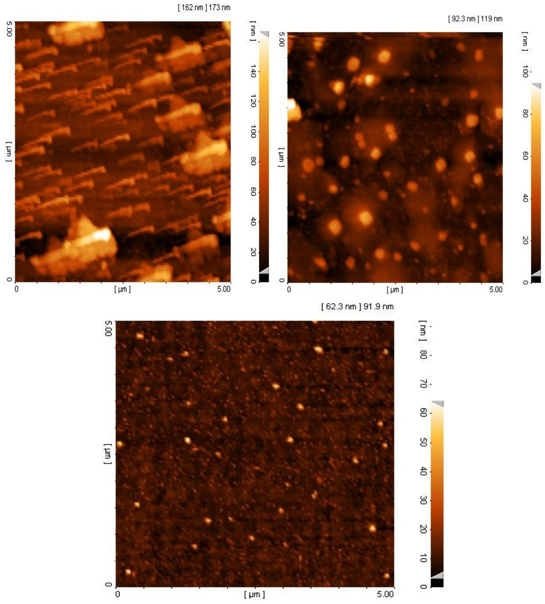

Figure 6 Figure 5 Figure 4

Figures 4, 5 and 6 show dimensional AFM images of the silicon deposition on glass substrates angles to the accumulation of 25 degrees, 35 degrees and vertically. As we see grains size in the vertical storage position (the piles) is bigger than others and finer grain size with increasing deposition angle between the grain and the holes s is even more so in effects of light will pass through them, and when angle increases further passing is better and reflection is less.

SEM images 8, 9 and 10 of the form accumulation of silicon shows angle of 25 degrees, 35 degree and vertically, respectively. In Figure 8 Angle increases the accumulation of grains that are larger and sharper.

As shown in Figure 9 tiny seed and gradually the seeds are bigger than others, fully consistent with the AFM images.

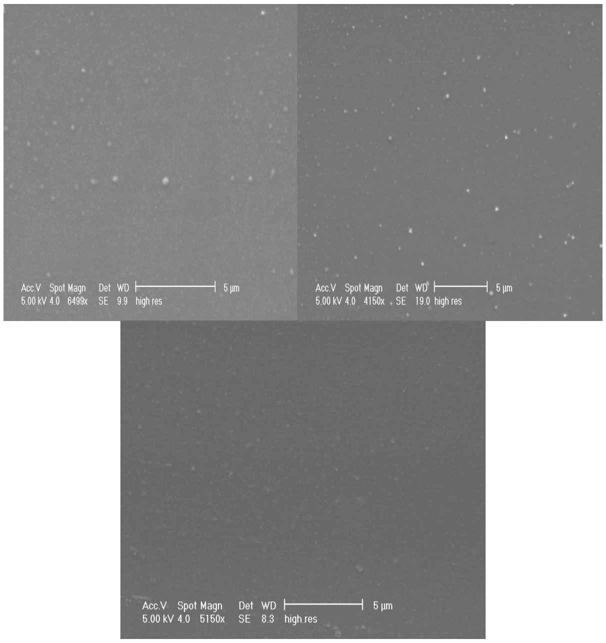

Figure 10 Figure 9 Figure 8

Figure 11 shows real parts of refractive index for the layers produced in this work with different thicknesses of 91.9 nm, 119 nm and 173 nm and other same deposition conditions. There is a peak at 3.4 eV energy for all layers by increasing thickness real part of refracting layers decreases with silicon grains and filling up the voids.

Figure 12 shows the imaginary part of refractive index. There is a peak at about 3.5 eV energy for all layers. As long as it can be seen from figure 2 by increasing thickness, imaginary part of refractive index increases that is because of filling voids with silicon grains, therefore, transmittance decreases and absorbance increases.

Figure 13 shows the real part of dielectric constant for our results, as it can be seen from figure 13, by increasing thickness real part of dielectric constant decreases. That is because of formation more metallic layers by increasing thickness also for thicker layers the effect of substrate are also observed.

Figure 14, shows the imaginary parts of dielectric constant. There is a peak at 3.5 eV energy for all layers. As it can be seen from figure 4, by increasing thickness, imaginary part of refractive index increases, that depends to more absorbance.

Figure 15 shows, the real part of conductivity index. The general trend and the peak at 3.4 eV energy are the same for all layers.

As it can be seen from figure 15, by increasing thickness, real part of conductivity index increases, that is because of formation completed metallic silicon layers and that is in agreement with figure 13 (real part of dielectric constant).

Figure 16 shows, the imaginary part of conductivity index. By increasing thickness, imaginary part of conductivity index decreases that depend to absorbance as we discussed before.

Figure 17 shows, absorption coefficient for the layers produced in this work. The general trend of all layers is the same. The peak at 3.4 eV is shown already. By increasing thickness absorption coefficient increases. That is because of formation of completed layers and filling up the voids with silicon metallic grains, therefor transmittance decreases and absorbance increases.

Figure 19 shows, real parts of refractive index for the layers produced in this work with different thickness.

Figure 20 shows real parts of refractive index for the layers produced in this work.

IV. SUMMERY

Silicon thin layers were deposited on glass substrates, under high vacuum condition, at room temperature (300K) with three different thicknesses by using of resistant evaporation method.

In AFM images of the silicon deposition we see grains size in the vertical storage position (the piles) is bigger than others and finer grain size with increasing deposition angle between the grain and the holes s is even more so in effects of light will pass through them, and when angle increases further passing is better and reflection is less. In SEM images of the form accumulation of silicon shows angle of 25 degrees, 35 degree and vertically increase the accumulation of grains are larger and sharper. The seeds that is bigger than others, fully consistent with the AFM image.

In this work by increasing thickness real part of refractive index decreases and imaginary parts of refractive index increases that was because of formation more completed layers and filling up the voids, that trends to decreasing transmittance and increasing absorbance. By increasing thickness real part of dielectric constant decreases and imaginary part of dielectric constant increases, for the same reasons there is an increasing and decreasing trend for real part and imaginary parts of conductivity constant respectively. Absorption coefficient increases by increasing thickness that we discussed before.

REFERENCES

[1] G. Binning, C. Quate and Ch. Gerber, Phys. Rev. Lett. 56, 930, 1986
[2] G. Binnig, H. Rohrer, CH. Gerber and E. Weibel, Phys. Rev. Lett. 49, 57, 1982
[3] G. Binnig and H. Rohrer, Reviews of Modern Physics 71, S324, 1999
[4] L. Eckertova: “Physics of thin films”, Plenum Press, 1977, chap. 2.
[5] S. Wolf, R.N. Tauber: “Silicon Processing for the VLSI Era”, Lattice Press, 1986. Vol.1, chap. 10.
[6] C.Y. Chang, S. Sze: “ULSI Technology”, McGrawHill, 1996. Chap. 8.
[7] S.H. Mohamed, M. Raaif, A.M. Abd El-Rahman and E.R. Shaaban, Properties of Rf Plasma Nitrided Silicon Thin Films at Different Rf Plasma Processing Powers, ACTA PHYSICA POLONICA A, 120 (2011) 552-557.
[8] Adam A. Filios, Yeong S. Ryu and Kamal Shahrabi, Optical Properties and Applications of Nanoscale Silicon, the Technology Interface Journal/Winter Special Issue 2009 , selected paper from the Proceedings of the IAJC-IJME 2008 ConferenceVolume 10 No. 2.
[9] A. Dima, F.G. Della Corte, C.J. Williams, K.G. Watkins, G. Dearden, N. O’Hare, M. Casalino, I. Rendina and M. Dima, Silicon nano-particles in SiO2 sol–gel film for nano-crystal memory device applications, Microelectronics Journal 39 (2008) 768–770.

FIGURE CAPTIONS

Figure 1: tridimensional AFM image of a deposition angle of 25 °
Figure 2: tridimensional AFM image of a deposition angle of 35 °
Figure 3: tridimensional AFM image of silicon substrate of a deposition angle of 90
Figure 4: dimensional AFM image of a deposition angle of 25 °
Figure 5: dimensional AFM image of a deposition angle of 35 °
Figure 6: dimensional AFM image of a deposition angle of 90 °
Figure 8: SEM images of silicon sample at an angle of 25 degrees
Figure 9: SEM images of silicon sample at an angle of 35 degree
Figure10: SEM images of vertically angle the silicon sample
Figure 11: The real part of refractive index of the layers with different thicknesses.
Figure12: The imaginary part of refractive index of the layers with different thicknesses.
Figure13: The real part of dielectric constant of the layers with different thicknesses.
Figure 14: The imaginary part of dielectric constant of the layers with different thicknesses.
Figure15: The real part of conductivity index of the layers with different thicknesses.
Figure16: The imaginary part of conductivity index of the layers with different thicknesses.
Figure17: Absorption coefficient of the layers with different thicknesses.
Figure 18: The refractive index of the layers with different thicknesses.
Figure 19: The transmission index of the layers with different thicknesses.

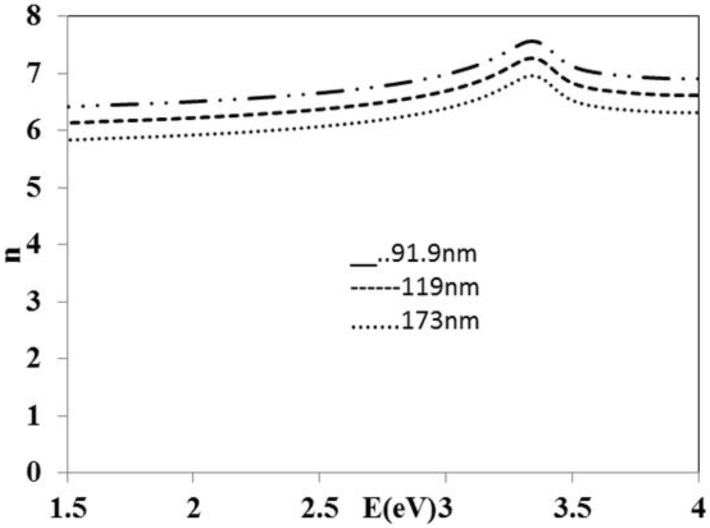

Figure 11: The real part of refractive index of the layers with different thicknesses

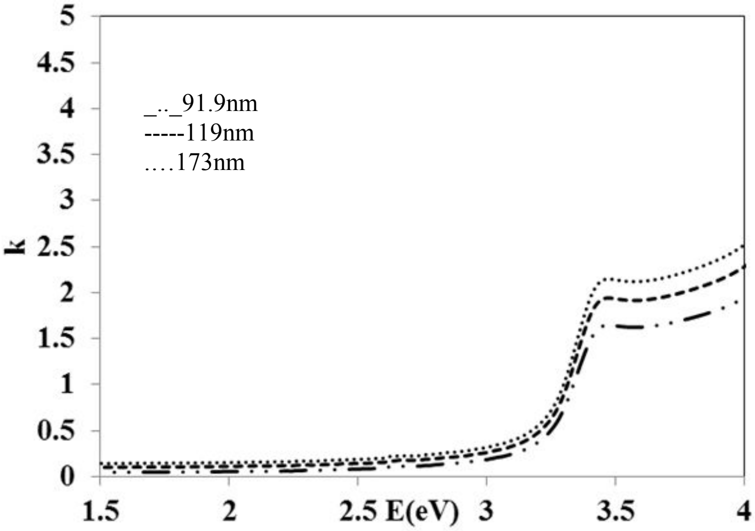

Figure12: The imaginary part of refractive index of the layers with different thicknesses.

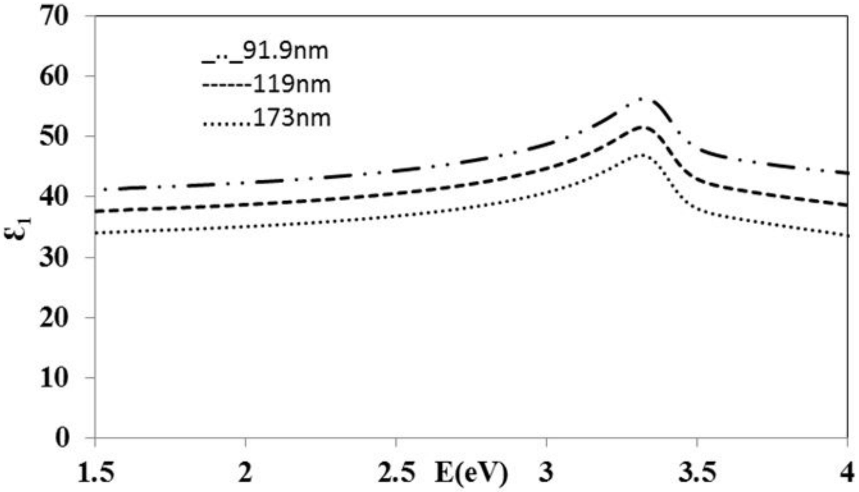

Figure13: The real part of dielectric constant of the layers with different thicknesses.

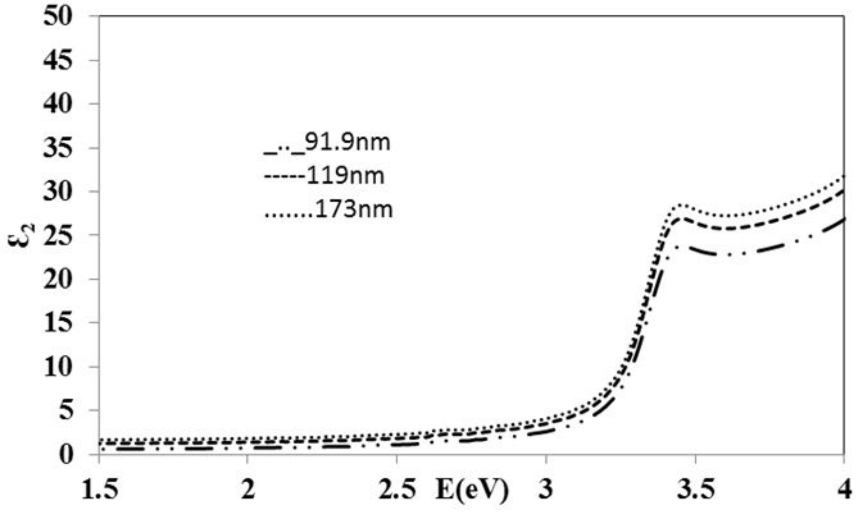

Figure 14: The imaginary part of dielectric constant of the layers with different thicknesses.

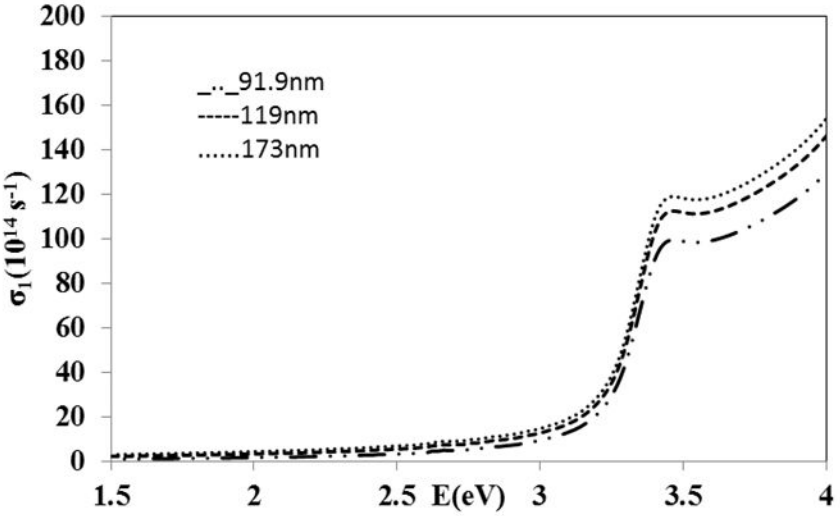

Figure15: The real part of conductivity index of the layers with different thicknesses.

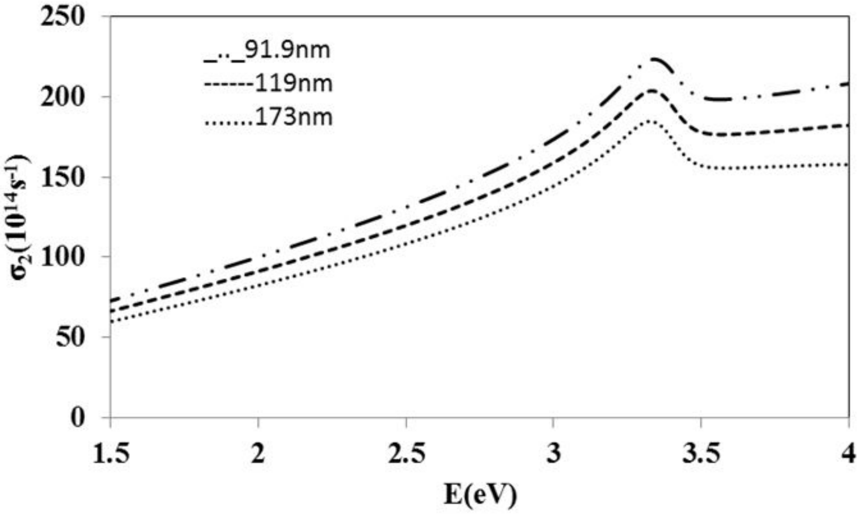

Figure16: The imaginary part of conductivity index of the layers with different thicknesses.

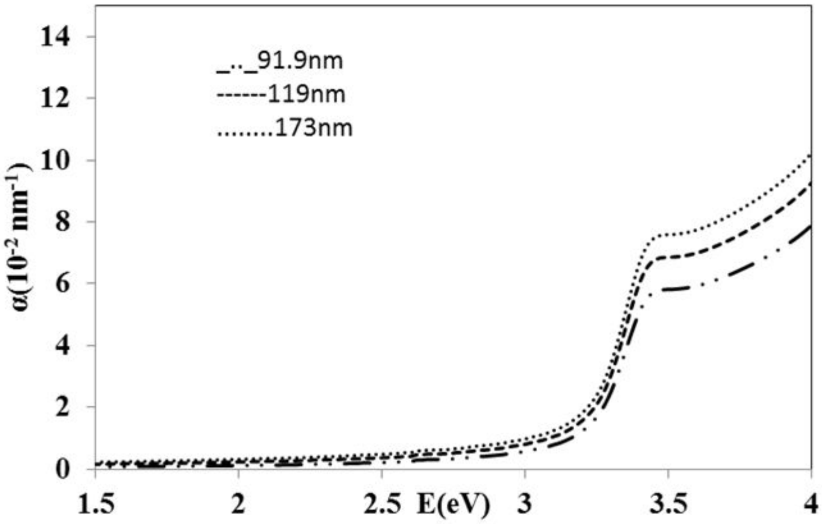

Figure17: Absorption coefficient of the layers with different thicknesses.

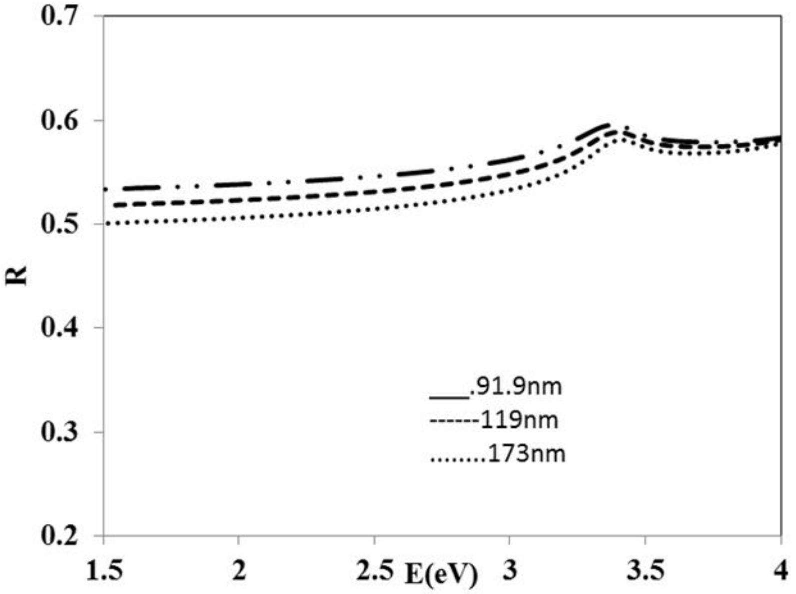

Figure 18: The refractive index of the layers with different thicknesses.

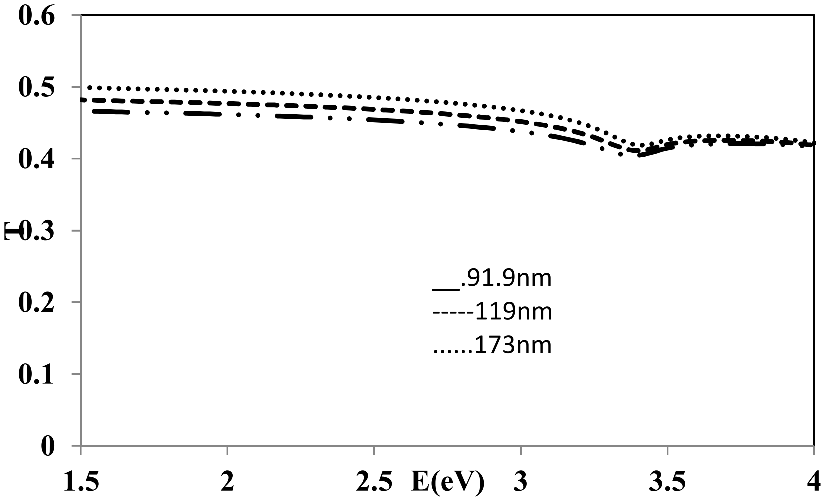

Figure 19: The transmission index of the layers with different thicknesses.